

FEASIBILITY STUDY OF MULTI-TURN ERL-BASED SYNCHROTRON LIGHT FACILITY

A.N. Matveenko^{*}, T. Atkinson, A.V. Bondarenko, Y. Petenev, Helmholtz-Zentrum Berlin, Germany

Abstract

Energy Recovery Linacs (ERL) have been discussed as drivers for synchrotron radiation facilities in X-ray region for over a decade. The first proposal for a multi-turn ERL as a next generation synchrotron light facility was in 1997 [1]. Since then great advances in ERL technology and high brightness electron source development were achieved [2], ERL-based high power free electron infrared laser at JLab (e.g. [3]) and the demonstration of multi-turn energy recovery at BINP [4]. The feasibility of an X-ray ERL-based light source seems more and more realistic.

An overview of the design of a multi-turn ERL under development at Helmholtz Zentrum Berlin (FSF – Femto-Science Factory) is given in this paper.

LAYOUT

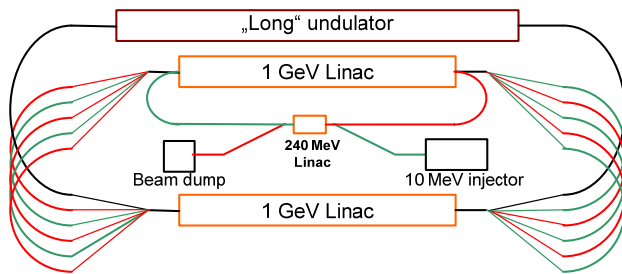


Figure 1: General layout of the FSF. Green lines – beam at acceleration, red – at deceleration, black – 6 GeV beam.

The accelerator layout is shown in the Fig. 1. It consists of a 10 MeV high brightness photo injector, medium energy (240 MeV in the picture) second stage injector, main linac, which is split into 2 1-GeV linacs (similar to CEBAF design). Each of the 1 GeV linacs is passed 3 times by the beam to gain 6 GeV, deceleration takes place in the reverse order. Undulators with user stations can be installed in (emittance optimized) arcs at all energies (see Fig. 4). Additionally, there is a possibility to have a long undulator at the maximal beam energy.

The beam and accelerator parameters are summarized in the following Table 1.

In following chapters we summarize specific features of this design.

Table 1: Main Parameters of the Multi-Turn ERL

Accelerator/beam parameters	High brilliance mode	Short pulse mode
E , GeV	6	6
$\langle I \rangle$, mA	20	5
Q_z , pC	15	4
$\epsilon_{\perp B}$, mm	0.1	~ 0.5
ϵ_{\parallel} , keV·mm	~ 3	~ 3
τ , fs	200-1000	~ 10
$\langle B \rangle$, $\frac{Ph}{s \cdot \text{mm}^2 \text{mrad}^2 0.1\%}$	$8 \cdot 10^{22}$	$\sim 4 \cdot 10^{21}$
B_{peak} , $\frac{Ph}{s \cdot \text{mm}^2 \text{mrad}^2 0.1\%}$	10^{26}	$\sim 10^{26}$

Two-Stage Injection and Split Linac Geometry

The cascade injection drastically improves the low to high energy ratio in the first 1 GeV linac, which allows for reasonable focusing along the linac for all energies and improves TBBU stability of the installation. On the other hand, 250 MeV arcs can be used for the longitudinal bunch compression (additional compression stage) on acceleration, to reduce the energy spread during deceleration by decompression, and to compensate for the average energy loss of the beam due to radiation. Finally, if one has concerns of even higher energy spreads at deceleration (consider SASE FEL), beam scrapers (or an additional beam dump for a reasonable average current) at 250 MeV can be thought of.

Split linac geometry allows to separate beams in the arcs, (i.e. the beam on accelerating path have different energy compared to the beam on the decelerating path) so that they are transported in separate vacuum chambers. This way all the beams can be steered separately, and users see only one beam type in every undulator.

Operation Modes

As shown in the Table 1, two main operational modes of the accelerator are considered. The high brilliance mode is optimized for the maximum average brilliance. Low transverse emittance and high flux are important for this mode. A long bunch is preferable in this mode to maximize the flux keeping transversal emittance low. No bunch compression is necessary, the linacs operate at phase 90° (maximal acceleration) of the RF, longitudinal dispersion (R_{56}) of all arcs are zero.

The short pulse mode is designed to provide short pulses of X-ray radiation with high peak brilliance. The bunch length in undulators is limited by collective effects in this case and will vary depending on the bunch charge.

^{*}Work supported by grants of Helmholtz Association VH-NG-636 and HRJRG-214

[#]aleksandr.matveenko@helmholtz-berlin.de

Bunch compression is distributed over 3 available compression stages: in the booster and merger; pre-injection linac and pre-injection arc; first turn in the main linacs, 1 and 2 GeV arcs. These arcs need to have adjustable longitudinal dispersion (R_{56}). The optimal distribution of the compression over the stages depends on the bunch charge and is subject to optimization.

Undulators

The parameters of the undulators investigated for the FSF are summarized in the Table 2. N is the number of periods, and N_{sec} is the number of undulator sections. Type 1 undulator is considered as “long undulator” for the 6 GeV return line. Type 2 undulators are considered for all arcs (5 undulator for each arc, up to 60 undulators in total).

Table 2: Undulator Parameters

Undulator parameters	Type 1	Type 2
N	3000	1000
N_{sec}	30	10
d , cm	4	4
K	0-2.5	0-2.5
B_{max} , T	0.67	0.67

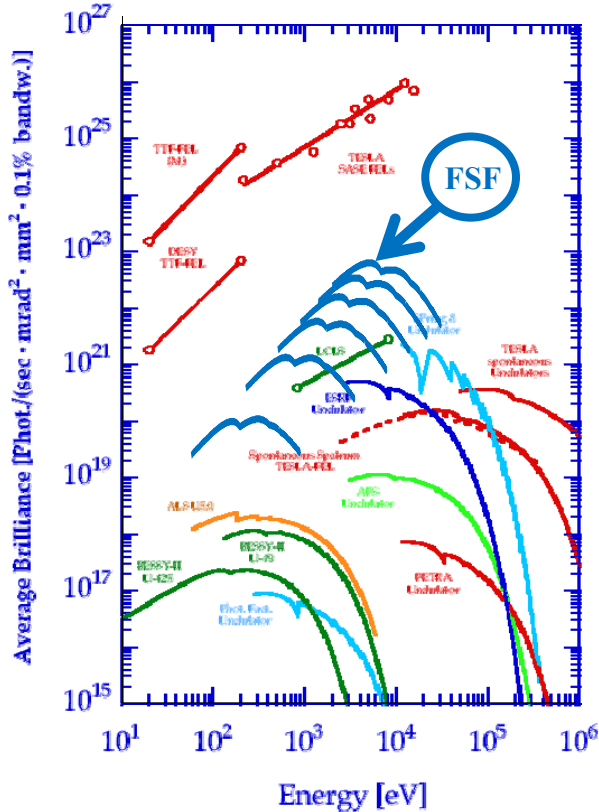


Figure 2: Brightness curves of the FSF arc undulators (Type 2 undulators of Table 2).

Coherent fraction of the radiation calculated according to [5] (see e.g. [6] for more detailed discussion)

$$\zeta = \frac{\lambda^2}{16\pi^2 \sigma_x \sigma_x' \sigma_y \sigma_y'}$$

is shown in Fig. 3. Transverse coherence approaching diffraction limit is achievable.

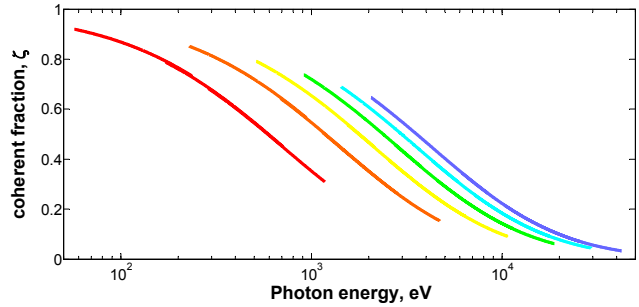


Figure 3: Coherent fraction of the FSF undulator radiation at 1 (red) through 6 (blue) GeV for the photon energies covered by the first to fifth harmonics.

Radiation Losses

The energy losses of the beam due to ISR, CSR, and other wakes are higher than the injection energy of the accelerator (see [11] for estimations in different operation modes). This energy must be compensated by booster linacs installed in the 6 GeV arc, or, alternatively, in the preinjector section with a separate high average power booster linac. Approximately 50 MeV and up to 500 kW losses should be compensated.

ACCELERATOR OPTIC ISSUES

Arcs

Each FSF arc consists of 6 30° bending sections and 5 undulators between them (Fig. 4).

Each bending section of the 3 to 6 GeV arcs (detailed layout shown in Fig. 5) is optimized to minimize the emittance growth due to both incoherent (ISR) and coherent synchrotron radiation (CSR). Each section consists of 4 identical triple-bend cells with matching quadrupoles to the following undulator (or spreader). An important feature of the cell design is the negative middle bend to achieve zero R_{56} at a moderate strength of quads. Each cell has betatron phase advance $Q_x=3/4$ in order to cancel out the emittance growth due to CSR [7] in each 30°-section. Twiss parameters inside cells are optimized to minimize the radiation integral I_5 .

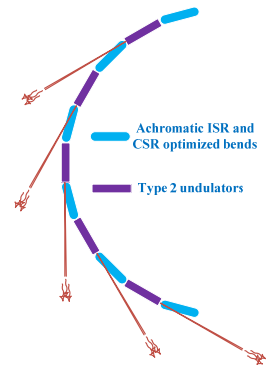


Figure 4: Layout of FSF arcs.

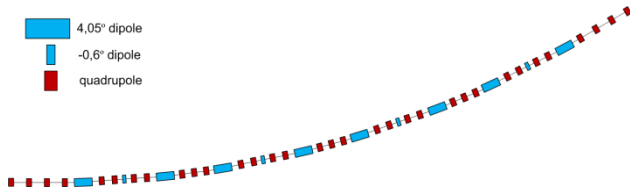


Figure 5: Layout of a 30°-section of the FSF arcs.

Bending sections of the 1 and 2 GeV arcs have a different design. Their contribution to the ISR emittance growth is small due to the low beam energy. On the other hand, they must have variable longitudinal dispersion for the beam compression in the short pulse mode. TBA cells are considered for these arcs.

Spreaders/Recombiners

The layout of the spreader at the entrance to linac 1 (which is identical to the recombiner at the exit of linac 1) is presented in the Fig. 7. The second pair of spreaders and recombiners is similar, but without the 6 GeV beam line, which goes to the long undulator section.

All spreader lines are isochronous.

One of the limiting factor for the spreader design is the contribution to the radiation integral I_5 , which characterizes the transversal emittance growth due to incoherent synchrotron radiation (see e.g. [8]).

$$I_5 = \int \frac{(y\eta'^2 + 2\alpha\eta\eta' + \beta\eta'^2)_ds}{|\rho|^3}$$

$$\Delta\varepsilon = \frac{2}{3} r_e C_q \gamma^5 I_5$$

Relatively high value of the horizontal β -function from the linac section limits the bending angle of the separating dipoles (which depicts η'). Quadrupoles are necessary to minimize the contributions of other dipoles to I_5 , which in combination with isochronous and reasonable β -functions conditions demands large numbers of them. Also a compact design is of advantage for the installation footprint.

The difficulties (which grow with the number of the beam energies to be separated) originate from the conditions on the β -functions (low I_5 contradicts with „natural“ β -functions of linacs), and dispersion (low I_5 contradicts with the beam lines separation). A Lambertson septum-like separation magnet for 4, 5, and 6 GeV beam lines (green in the Fig. 7) helps to significantly reduce the distances necessary for the beam separation. The optic of the spreader is coupled in this case, which complicates the analysis and ongoing optimization.

Linacs

The focusing optic in linacs can be added quite naturally between cryomodules. The options include triplets, doublets, single quadrupoles, or no additional elements at all. It was argued [9], that the additional focusing does not change maximal β -functions in the linacs significantly. For a multi-turn ERL, however, we consider the transversal beam break-up (TBBU) to be a serious problem and hold the optic optimization in the

linac for important. The option with triplets of quadrupoles between cryomodules seems most promising in our case, although the effect is of the order of 2-3 times larger in the TBBU threshold current.

β -functions in linacs are shown in Fig. 8. For the details of TBBU modeling and comparison of different injection schemes in this respect see [10].

Start-to-end Beam Dynamics Simulation

Comprehensive results of the FSF start-to-end beam dynamics modeling are presented in [11], here is a summary.

ASTRA simulations are used to track the space charge dominated beam from the photo-injector, through the Booster and Merger to the entrance of the 230 MeV pre-injector linac. Subtle beam transformation through the injection stage is used to produce a low emittance beam in all six dimensions. From here onwards, Elegant was used to optimize and track the beam during acceleration to 6 GeV and the deceleration recovery to the dump transfer line.

For the LEM the transverse emittance growth is kept to a minimum throughout the whole 7 km machine Fig. 6 to maximize user potential.

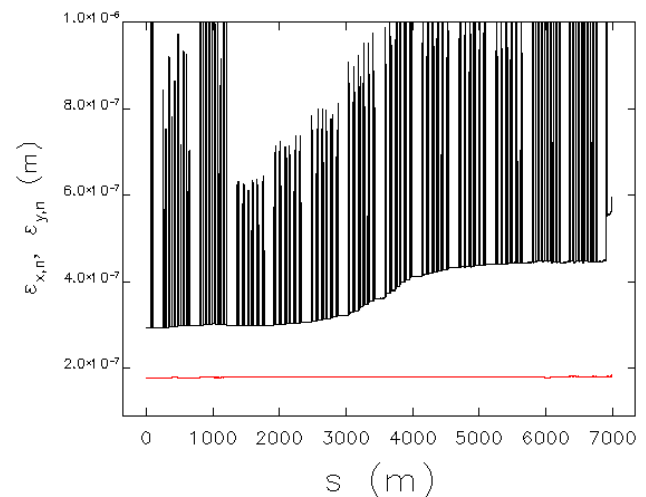


Figure 6: Normalized emittance plot for LEM.

The emittance growth is mainly due to incoherent radiation effects and can be estimated for the final energy arc as $\Delta(\gamma\varepsilon) = 4 \cdot 10^{-8} E^6 I_5 \sim 0.04$ mm mrad.

Multipoles were implemented in the low energy arcs to recover the longitudinal emittance of the injector during bunch compression. Either side of off-crest acceleration in both linacs ($\phi_1=10^\circ$, $\phi_2=-20^\circ$) combined with longitudinal dispersive optic ($R_{56}=20$ cm, $R_{56}^{\prime}=5$ cm) telescopic optic produces a 10 fs short bunch at the 6 GeV long undulator section. Fig. 9 shows the recovery of the normalized emittance (black) and the bunch length (red) throughout the machine. The slow emittance growth and the bunch (de)compression asymmetry are due to radiation effects.

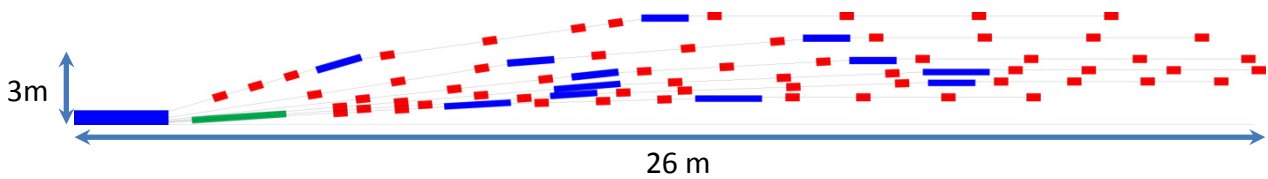


Figure 7: Layout of the spreader section behind the linac1.

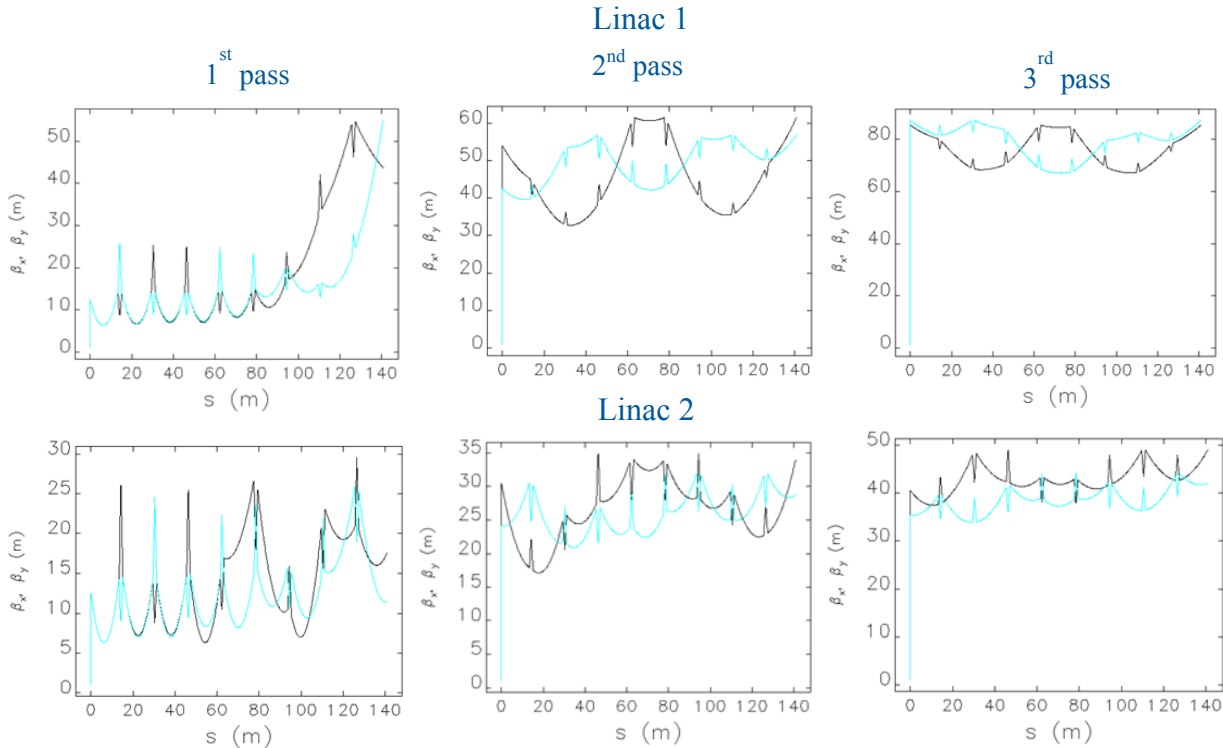


Figure 8: β -functions in linacs. Final energies in the first linac are 1, 3, and 5 GeV; in the second – 2, 4, and 6 GeV. Triplet-based optic common for all beams in each linac is optimized for minimal β -functions.

Simulation results of the recovered beam at the entry to the beam dump transfer line are given in Table 3. Although the energy spread of the beam in both modes at the entrance to the dump line is approximately 5%, the beam could be safely transported to the dump using a low dispersive optic.

CONCLUSION

An overview of the design of a multi-turn ERL (FSF – Femto-Science Factory) is given in this paper. Due to the availability of many (6) beam energies in the facility, a broad spectral region of synchrotron radiation (50 eV to 50 keV) is covered with ultimate photon beam brilliance reaching diffraction limit.

The facility will provide the possibility to generate very short (down to 10 fs) photon pulses with high peak brilliance and high pulse repetition rate (1.3 GHz).

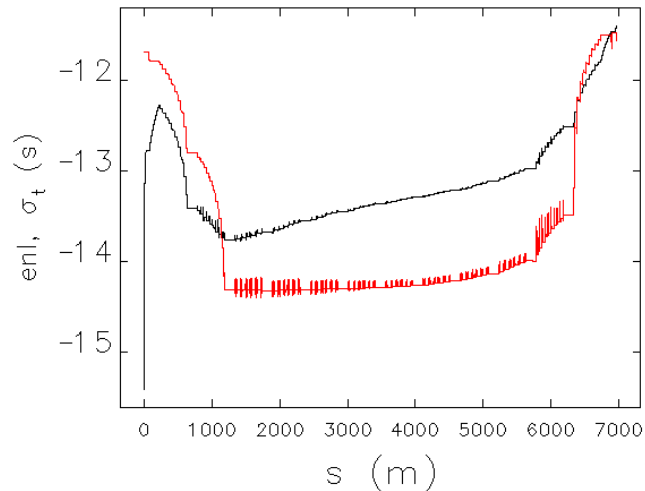


Figure 9: Log plot of the longitudinal bunch properties.

Table 3: Simulation Results at the Beam Dump Entrance

Type	ε_{nx} (mm mrad)	ε_{ny} (mm mrad)	St (ps)	DE/E (%)	Charge (pC)
SPM	0.48	0.20	2.24	3.76	1
LEM	0.36	0.18	4.02	7.60	15

REFERENCES

- [1] D.A. Kayran, et. al., "MARS –A Project of the Diffraction Limited Fourth Generation X-ray Source", Proc. of 1998 Asian Particle Accelerator Conference.
- [2] B. Dunham, et al., "Performance of the Cornell High-Brightness, High-Power Electron Injector", IPAC 2012, New Orleans, Louisiana (May 2012)
- [3] S. Benson et al, High power lasing in the IR upgrade at Jefferson Lab, Proc. 2004 FEL Conf., 229-232.
- [4] N.A. Vinokurov et al., Status and prospects of the Novosibirsk FEL facility, Proc. RuPAC'10, pp.133-135.
- [5] X-ray data booklet, available online at <http://xdb.lbl.gov/>, section 2_1.
- [6] I.V.Bazarov, PRST AB 15, 050703 (2012).
- [7] J.Wu, et al., "Coherent Synchrotron Radiation Analysis for the Photoinjected ERL and UVFEL Projects at NSLS", Proc. of 2001 Particle Accelerator Conf., pp.2866-2868.
- [8] M. Sands, "The physics of electron storage rings. An introduction", Proc. of the International School of Physics "Enrico Fermi", ed. B. Touschek, (Academic Press, 1971).
- [9] V.Litvinenko, private communication.
- [10] Y.Petenev, T. Atkinson, A.V. Bondarenko A.N. Matveenko, Analysis of Injection and Recovery Schemes for a Multi-turn ERL based Light Source, Proc. of 53th ICFA Advanced Beam Dynamics Workshop on Energy Recovery Linacs, Novosibirsk, 2013.
- [11] T. Atkinson, A.V. Bondarenko, A.N. Matveenko, Y.Petenev, Start-to-end beam dynamics simulations for Femto-Science-Factory feasibility study, Proc. of 53th ICFA Advanced Beam Dynamics Workshop on Energy Recovery Linacs, Novosibirsk, 2013.